JMEPEG (2012) 21:2535–2545
DOI: 10.1007/s11665-012-0375-0
©ASM International
1059-9495/$19.00

Phase Transformation Behavior of Hot Isostatically Pressed NiTi-X (X = Ag, Nb, W) Alloys for Functional Engineering Applications

M. Bitzer, M. Bram, H.P. Buchkremer, and D. Stöver

(Submitted March 5, 2012; in revised form August 16, 2012)

Owing to their unique properties, NiTi-based shape memory alloys (SMAs) are highly attractive candidates for a lot of functional engineering applications like biomedical implants (stents), actuators, or coupling elements. Adding a third element is an effective measure to adjust or stabilize the phase transformation behavior to a certain extent. In this context, addition of alloying elements, which are low soluble or almost insoluble in the NiTi matrix is a promising approach and—with the exception of adding Nb—has rarely been reported in the literature so far, especially if the manufacturing of the net-shaped parts of these alloys is aspired. In the case of addition of elemental Nb, broadening of hysteresis between austenitic and martensitic phase transformation temperatures after plastic deformation of the Nb phase is a well-known effect, which is the key of function of coupling elements already established on the market. In the present study, we replaced Nb with additions of elemental Ag and W, both of which are almost insoluble in the NiTi matrix. Compared with Nb, Ag is characterized by higher ductility in combination with lower melting point, enabling liquid phase sintering already at moderate temperatures. Vice versa, addition of W might act in opposite manner considering its inherent brittleness combined with high melting temperature. In the present study, hot isostatic pressing was used for manufacturing such alloys starting from prealloyed NiTi powder and with the additions of Nb, Ag, and W as elemental powders. Microstructures, interdiffusion phenomena, phase transformation behaviors, and impurity contents were investigated aiming to better understand the influence of insoluble phases on bulk properties of NiTi SMAs.

Keywords hot isostatic pressing (HIP), NiTi Ag, NiTi Nb, NiTi W, phase transformation temperatures, Powder metallurgy, Shape memory

1. Introduction

Owing to their unique mechanical behavior, shape memory alloys (SMAs) are highly attractive to be used as functional materials like actuators or coupling elements (Ref 1-3). Especially, NiTi alloys with near-equiatomic composition have attained increasing interest considering their reversible shape recovery up to 8% (Ref 4). The reversible martensite-austenite transformation takes place in the temperature range from −50 to 110 °C as a function of the Ni-content of the matrix (usually 48-51 at.%) (Ref 5).

Adding a third element might influence the phase transformation behavior significantly and is thereby able to enlarge the application field of the alloys. During the last decade, many investigations were carried out on ternary NiTi-X alloys with X = Mo, Al, Hf, Co, Cr, Cu, V, Mn Fe, Pd, Pt, or Au. All of them show phase transformation behavior, shape memory effect (SME), and superelasticity (SE) as known from binary NiTi-alloys (Ref 6-12). In these cases, the third element replaces either Ni or Ti atoms in the intermetallic NiTi lattice. Suitable candidates for a reduction of the phase-transformation temperatures are Cr, V, or Mn as substitution of Ti or Co and Fe as substitution of Ni. Vice versa, an increase of the temperatures can be achieved by adding Au, Pd, or Pt as substitution of Ni or Zr and Hf as substitution of Ti (Ref 12). Furthermore, a stabilization of the phase transformation temperatures can be achieved by adding elements like Cu (Ref 12).

In contrast to the above mentioned NiTi-X alloys, the addition of third alloying elements, which are low soluble or almost insoluble in the NiTi matrix, is quite exceptional. A well-known example for this approach is the addition of elemental Nb (Ref 14-16), which is already established in the production of coupling elements on an industrial scale (Ref 17). For this application, low M_S temperature and broad hysteresis of phase transformation temperatures are required, so that A_S and M_S differ as far as possible. Low M_S temperatures maintain good mechanical stability and high clamping forces even at low application temperatures so that it is guaranteed that the couplings remain in the austenitic state throughout their service life. Otherwise, a beginning transformation to the martensite would result in a reduced yield stress and in the worst case, the component's failure. High A_S temperatures avoid premature

This article is an invited paper selected from presentations at the International Conference on Shape Memory and Superelastic Technologies 2011, held November 6-9, 2011, in Hong Kong, China, and has been expanded from the original presentation.

M. Bitzer, M. Bram, H.P. Buchkremer, and **D. Stöver**, Institute for Energy and Climate Research (IEK-1: Materials synthesis and processing), Forschungszentrum Jülich GmbH, 52425 Jülich, Germany. Contact e-mail: m.bitzer@fz-juelich.de.

shrinkage even up to high ambient temperatures and determine the maximum storage temperature. The M_S temperature required for a specific application load can be calculated by Eq 1 (Ref 13).

$$M_S^* < T_0 - \sigma_r(d\sigma/dT)^{-1} \quad \text{(Eq 1)}$$

where T_0 is the lowest expected service temperature, σ_r is the minimum recovery stress needed for the clamp effect, and $d\sigma/dT$ is the stress rate of the alloy, for NiTi typically 5 MPa/°C. For most applications, an M_S temperature below −90 °C is required (Ref 13).

In the case of NiTi-Nb alloys, the shift of the martensite transformation to extremely low temperatures is caused by an excess of Ni in the NiTi matrix, as realized in the well-established alloy composition, $Ni_{47}Ti_{44}Nb_9$ (in at.%), usually applied for coupling elements (Ref 13-15). Broadening of hysteresis is supported by partial solubility of Nb in the NiTi matrix. Zhao et al. (Ref 18) showed that the solubility of Nb in NiTi matrix increases with Ni-content. In this study, Nb contents in NiTi matrix varied from 2.3 to 4.9 at.% depending on alloy composition. Excess of Nb has been found as homogenously distributed, ductile Nb-based inclusions. Analysis of phase transformation temperatures leads to the conclusion that amount of Nb dissolved in the NiTi matrix is predominant for broadening of hysteresis and not necessarily high amount of isolated Nb particles. Diffusion of Ti into the Nb phase further contributes to enhancing Ni content of the NiTi matrix and therefore broadening of hysteresis.

Shifting A_S to higher values is mainly based on predeformation in martensitic state. Owing to the deformation, the martensite of the NiTi-matrix is detwinned using preferred variants in load direction, while the Nb-phase is deformed plastically. When transforming back to the austenite by heating, the Nb-phase hinders the shape recovery process providing a frictional stress to the NiTi matrix. Additional energy required for the redeformation of the ductile Nb phase results in an increased A_S temperature. For this process it is essential that the stress level of the martensitic plateau is approximately 50 MPa higher than the yield strength of the Nb phase (approximately 200 MPa). The shift of A_S due to ductile phases in pre-deformed alloys can be calculated by the Clausius-Clapeyron Eq 2 (Ref 13).

$$\Delta A_S = \sigma_f^{Nb}(d\sigma/dT)^{-1} \quad \text{(Eq 2)}$$

If the yield strength of Nb is assumed as σ_f^{Nb} = 200 MPa and the recovery stress for NiTi as 5 MPa/°C, then a shift of ΔA_S of 40 °C is expected. In sum, temperature hysteresis of 72.5 °C is calculated for Ni47Ti44Nb9 alloy, which is established for application in coupling devices (Ref 18).

A less-pronounced effect also inducing broadening of hysteresis can be already found in undeformed NiTi-Nb alloys. It has been proposed that in the case of martensitic phase transformation, the presence of Nb particles in the NiTi matrix facilitates the accommodation of the surrounding martensite phase because of the introduction of small local deformations in the Nb phase at the martensite-Nb interface. As a consequence, during subsequent heating, martensite becomes stabilized in the vicinity of the Nb phase, which even tends to shift the A_S temperature to higher values (Ref 17). As an example, Bansiddhi et al. (Ref 16) reported an increase of temperature hysteresis in undeformed, powder metallurgical Ni48.6Ti51.4 alloy with temperature ranging from 42 to 55 °C when adding 3 at.% Nb, which might be explained by this phenomenon.

Up to now, less information on ternary NiTi-X alloys is given in the literature as regards Nb being replaced by the addition of elemental Ag or W. Contrary to Nb, both the latter elements are almost insoluble in the NiTi lattice. In the case of Ag, solubility <0.1 at.% was reported by Oh et al. (Ref 19). Solubility of W was discussed in the literature to be slightly higher [<0.3 at.% (Ref 20), <0.9 at.% (Ref 21)]. Therefore, the influence of interdiffusion phenomena and solid solution effects on phase transformation behavior can be almost neglected. Furthermore, it is expected that the effectiveness of Ag and W is quite different from Nb, as elemental Ag is characterized by its higher ductility compared with Nb, while W tends to behave rather brittle. Furthermore, large differences in melting points (NiTi: 1310 °C, Ag: 961 °C, W: 3422 °C, compared with Nb: 2468 °C, but the formation of eutectic melt of Nb with NiTi at temperatures above 1170 °C (Ref 16, 22)) is expected to influence the processing of NiTi-Ag and NiTi-W alloys clearly.

The production of these alloys by conventional arc- or induction melting is quite difficult as strong tendency of segregation is caused by the above mentioned differences in melting points as well as densities (NiTi: 6.45 g/cm^3, Ag: 10.49 g/cm^3, W: 19.30 g/cm^3, Nb: 8.57 g/cm^3). Nevertheless, production of NiTi-1W and NiTi-2W alloys by arc melting was reported by Hsieh et al. (Ref 23). Recently, NiTi-Ag and NiTi-W coatings were produced by DC magnetron sputtering from elemental targets enabling deposition of continuous composition spread type materials libraries of both alloying systems (Ref 24-26).

In the present study, NiTi-Ag and NiTi-W alloys were prepared by powder metallurgical means using hot isostatic pressing (HIP) starting from prealloyed NiTi powders, which were blended with elemental Ag and W powders. The amounts of Ag and W were varied by 3 and 9 at.%, respectively. The prealloyed NiTi powder used in this study was enriched in Ni (50.8 at.%) to shift M_s to lower temperatures, supporting the broadening of hysteresis as discussed before. As reference, samples of binary NiTi powders as well as NiTi-Nb samples with 3 and 9 at.% Nb were prepared by the same method. During cooling from HIP temperature, residual stresses on the alloying phase might result from the mismatch of thermal expansion coefficients (TEC) to the NiTi matrix [α(NiTi, austenite): 11.0×10^{-6} K^{-1} (Ref 27), α(NiTi, martensite): 6.6×10^{-6} K^{-1} (Ref 27), α(Nb): 7.2×10^{-6} K^{-1} (Ref 28), α(Ag): 19.1×10^{-6} K^{-1} (Ref 29), α(W): 4.5×10^{-6} K^{-1} (Ref 30)]. Considering TEC values, tensile stresses will occur in the NiTi matrix at the NiTi-Ag interface. In contrast, W particles will lead to compression stresses in the NiTi matrix at the NiTi-W interface. Stress relaxation might occur by formation of dislocations at the interface.

HIP technology is promising for processing of NiTi-Ag and NiTi-W alloys as superposition of pressure during sintering supports densification up to almost theoretical density while eliminating the influence of residual porosity on specific properties. HIP enables the net-shaped production of parts with moderate geometrical complexity like tubes or cylinders. In combination with electro-discharge machining (EDM), the manufacturing of coupling rings and tensile samples becomes possible, which can be used for comprehensive characterization of these alloys. As HIP in combination with EDM is limited regarding large scale production, transfer to net-shape manufacturing by metal injection molding (MIM) is in progress. Here, especially, the addition of Ag as third alloying element seems to be quite promising. The possibility of liquid-phase sintering at

moderate temperatures enables us overcome the drawback of low sintering activities of binary NiTi powders in the case of pressureless sintering. In our previous studies, residual porosities of net-shaped NiTi parts made by MIM in the range of 3-10% remained after sintering (Ref 31-33). Following the trend, Ni-rich NiTi alloys showed higher sintering activity resulting in lower residual porosity at given sintering temperature. Alloying with W is expected to behave worse during MIM processing, as almost negligible interdiffusion between W and NiTi and low sintering activity of W powders at temperatures far below the W melting point may lead to even higher porosities than those achieved for binary NiTi alloys.

2. Experimental

2.1 Starting Materials

In the present study, prealloyed NiTi powder was used, which was manufactured by TLS Technik GmbH & Co Spezialpulver KG (Bitterfeld, Germany) using electrode induction inert gas atomization (EIGA) of commercial NiTi rods (Special Metals, New Hartford, USA) with nominal Ni-content of 50.8 at.%. The morphology of the prealloyed NiTi powder is shown in Fig. 1(a). Elemental Nb, Ag, and W powders (Alfa Aesar GmbH & Co KG, Karlsruhe, Germany) were used as alloying elements (Fig. 1b-d). Particle size distributions of starting powders are summarized in Table 1. The d_{10}, d_{50}, and d_{90} values in this table represent the particle diameters of the starting powders before blending, where 10, 50, and 90 mass% of the powder particles, respectively, have a smaller equivalent diameter. Impurity contents (oxygen, carbon) of the starting powders are given in Table 2.

2.2 Alloying Process and Hot Isostatic Pressing of the NiTi-X Alloys

Prealloyed Ni50.8Ti49.2 powder was blended with elemental Nb, Ag, or W powders. Amounts of alloying phase were kept constant at 3 and 9 at.% (nomenclature NiTi-3Nb, NiTi-9Nb, NiTi-3Ag, NiTi-9Ag, NiTi-3W, NiTi-9W). For improving the homogeneity, blending was done in a turbula mixer for 4 h, while adding zirconia balls and ethanol. After mixing, balls were removed, and powders were dried in a heated cupboard. For load transfer during HIP, powder mixtures were encapsulated in cylindrical steel capsules (material 1.4571) with an outer diameter of 18 mm, a wall thickness of 1 mm, and a length of 70 mm. To avoid segregation during capsule filling as well as excessive deformation of the capsules during HIP, the powder mixtures were precompacted by uniaxial pressing at 60 MPa. Afterward, the capsules were welded by electron beam in vacuum. The HIP process was performed at temperature of 1065 °C, pressure of 100 MPa and dwell time of 3 h. The pressure was applied by Argon gas. The heating- and cooling rates were 15 K/min. After HIPing, the capsules were removed by mechanical machining. HIP sample made of binary Ni50.8Ti49.2 powder was produced as reference using the same parameter set. To avoid uncontrolled precipitation of metastable Ni_4Ti_3 phase in the NiTi matrix, which would be coupled with occurrence of additional R-phase transformation (Ref 33), all samples were solution treated at 950 °C for 1 h followed by water quenching.

To demonstrate the potential of powder metallurgical NiTi-X (X = Nb, Ag, W) alloys for real application, coupling rings were cut from HIPed samples by EDM. The rings had an outer diameter of 9 mm, an inner diameter of 6 mm, and a height of 3 mm. To establish their clamping ability, rings were widened up to 6 and 12% (related to the inner diameter) by pressing them in liquid nitrogen over a mandrel.

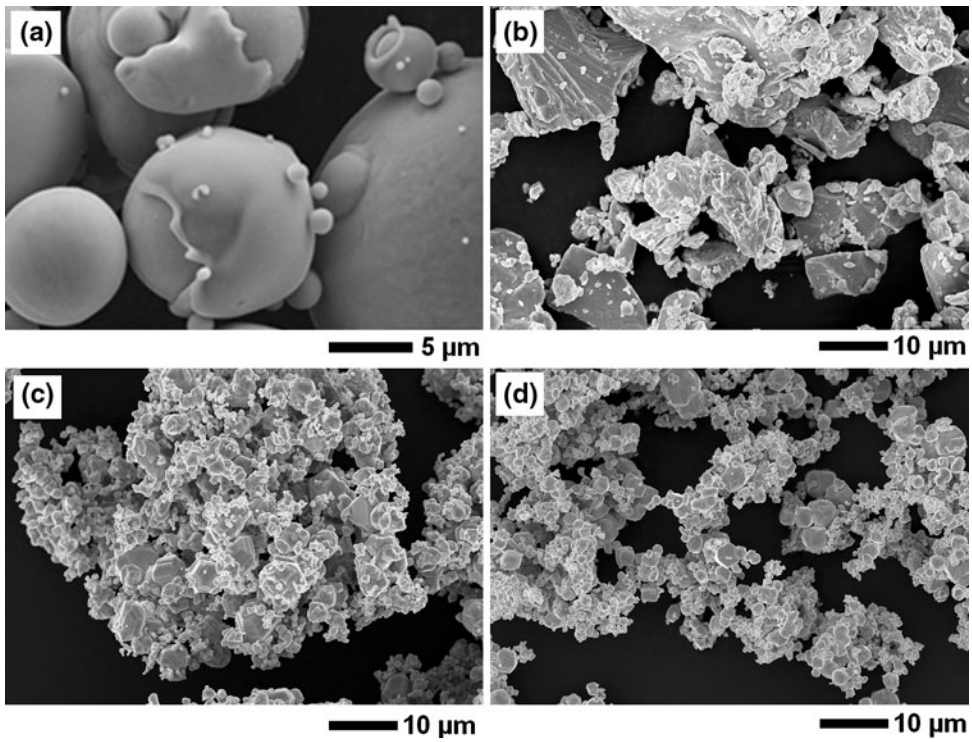

Fig. 1 Morphology of the starting powders. (a) Prealloyed Ni50.8Ti49.2 powder, (b) Nb powder, (c) Ag powder, and (d) W powder

Table 1 Particle size distributions of the starting powders

Powder	Particle size		
	d_{10}, µm	d_{50}, µm	d_{90}, µm
Ni50.8Ti49.2	8	16	36
Nb	6	11	20
Ag	9	14	22
W	5	8	12

Table 2 Comparison of impurity contents (oxygen and carbon) of starting powders and of NiTi- and NiTi-X (X = Nb, AG, and W) samples after HIP compaction (n = 5 for each measurement)

Sample	Oxygen, wt.%	Carbon, wt.%
Ni50.8Ti49.2 (powder)	0.0532 ± 0.0017	0.0291 ± 0.0020
Nb (powder)	0.7793 ± 0.0016	0.0072 ± 0.0007
Ag (powder)	0.0288 ± 0.0045	0.0029 ± 0.0021
W (powder)	0.0778 ± 0.0028	< 0.0010
Ni50.8Ti49.2 (HIP)	0.0485 ± 0.0011	0.0328 ± 0.0032
NiTi-3Nb (HIP)	0.0882 ± 0.0022	0.0333 ± 0.0023
NiTi-9Nb (HIP)	0.1692 ± 0.0025	0.03293 ± 0.0077
NiTi-3Ag (HIP)	0.0518 ± 0.0018	0.0347 ± 0.0018
NiTi-9Ag (HIP)	0.0504 ± 0.0015	0.0368 ± 0.0030
NiTi-3W (HIP)	0.0595 ± 0.0020	0.0334 ± 0.0042
NiTi-9W (HIP)	0.0747 ± 0.0031	0.0264 ± 0.0036

2.3 Characterization

After metallographical preparation, microstructures of all samples were investigated by scanning electron microscopy (SEM, Zeiss Ultra 55) in combination with qualitative energy-dispersive X-ray spectroscopy (EDX). Phase transformation temperatures were determined by differential scanning calorimetry (DSC, TA Instruments, 2920 MDSC) with heating and cooling rates of 10 K/min in the temperature range −100 and +100 °C. Oxygen contents were analyzed by inert gas fusion infrared method and carbon contents by combustion infrared absorption method. Density measurement of samples was conducted by Archimedes method.

3. Results

3.1 Impurity Contents and Densities After HIP Compaction

In the case of HIP processing, impurity contents of NiTi and NiTi-X alloys are mainly introduced already by the starting powders. During HIP, gastight encapsulation of powders under vacuum avoids further contamination reliably (Ref 33-35). As solubility of oxygen and carbon is almost negligible in the NiTi matrix, uptake of these elements lead to the formation of oxygen-containing Ti_2Ni-phase (in the literature often named "$Ti_4Ni_2O_x$") and TiC (Ref 5, 36). Compared to the starting powders, coarsening of both phases was found after HIP. Phases tend to be located preferentially on former NiTi powder particle surfaces. This arrangement clearly influences mechanical properties and fracture behavior (Ref 32, 34). Furthermore, both phases remove Ti from the NiTi matrix, which leads to decrease of phase transformation temperatures following the well-known curves published by Tang et al., Khalil-Allafi et al., or Frenzel et al. (Ref 5, 37, 38). When alloying binary NiTi alloys with elemental powders characterized by low or almost negligible solubility in the NiTi matrix, these powders may act as an additional source for increasing oxygen and carbon contents. In the present study, a clear relationship between the amount and the impurity contents of the elemental powders and the resulting impurity contents of the HIPed sample was found (Table 2). A discussion, how these additional impurities might change the distribution of oxygen-containing Ti_2Ni and TiC phase in the NiTi matrix is given later.

Table 3 Densities of NiTi and NiTi-X alloys (X = Nb, Ag, W) after consolidation by HIP (1065 °C, 100 MPa, 3 h) measured by Archimedes method (n = 3 for each sample)

Sample	Density, g/cm^3	Theoretical density, g/cm^3
Ni50.8Ti49.2	6.347 ± 0.012	6.45
NiTi-3Nb	6.525 ± 0.011	6.56
NiTi-9Nb	6.689 ± 0.002	6.76
NiTi-3Ag	6.604 ± 0.008	6.60
NiTi-9Ag	6.874 ± 0.003	6.89
NiTi-3W	6.922 ± 0.004	6.89
NiTi-9W	7.752 ± 0.006	7.76

Theoretical density of ternary alloys was calculated by rule of mixture

The densities of powder metallurgical NiTi- and NiTi-X (X = Nb, Ag, W) alloys consolidated by HIP were measured using the Archimedes method (Table 3). Clear deviations from theoretical densities were only observed for Ni50.8Ti49.2 as well as for NiTi-3Nb and NiTi-9Nb, indicating residual porosities in the range between 0.5 and 1.6%. As we did not see any pores in the microstructure of related samples, the reason of deviation especially in the case of binary NiTi is still unclear. For NiTi-Nb alloys, exact calculation of theoretical density was hindered by the fact that densities of apparent phases are influenced by interdiffusion of Nb into NiTi matrix as well as Ti into Nb phase, which tends to be more pronounced in the case of powder metallurgical production based on solid-state diffusion compared to ingot metallurgy.

3.2 Binary NiTi as Reference

As reference, binary Ni50.8Ti49.2 samples were produced by HIP using same parameter set as for ternary NiTi-X alloys. Figure 2 summarizes the influence of powder metallurgical processing on the phase transformation behavior of this alloy, which confirmed the results of previous studies (Ref 32-34). From our experience, measurement of phase transformation temperatures of prealloyed NiTi powders produced by gas atomization does not have high significance as these powders are far from thermodynamic equilibrium considering the rapid solidification of NiTi melt after passing the atomization nozzle. Ni:Ti ratio of each powder particle depends strongly on its specific solidification rate and impurity content, both of which are expected to vary significantly with particle size. Consequently, phase transformation peaks were broadened, furthermore indicating the occurrence of R-phase transformation (Fig. 2a). HIP under given conditions is an effective means to equalize deviations of Ni:Ti ratio of NiTi starting powders by solid-state diffusion process. Nevertheless, even in the as-HIPed state, reproducibility of phase transformation behavior

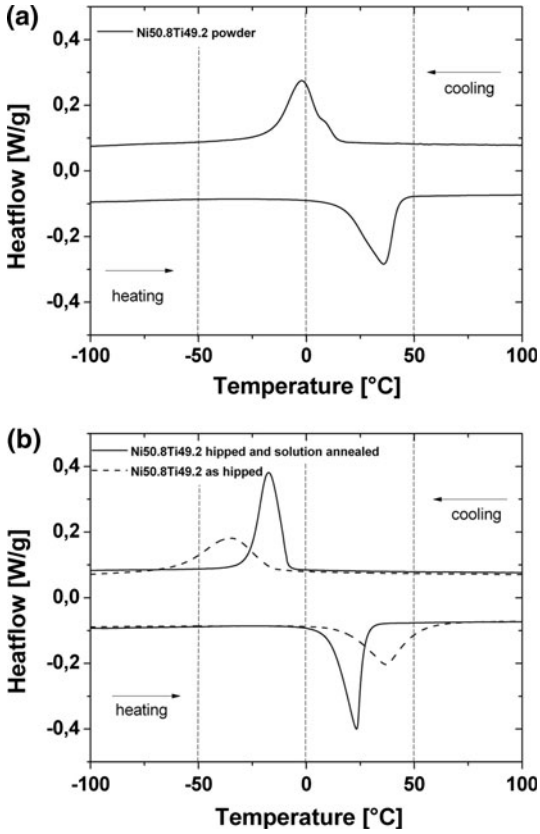

Fig. 2 Phase transformation behavior of Ni50.8Ti49.2 measured by DSC:. (a) Starting powder, and (b) after consolidation by HIP (1065 °C, 100 MPa, 3 h) without and with solution treatment (950 °C, 1 h, water quenching)

of Ni-rich NiTi alloys must be doubtful as uncontrolled precipitation of metastable Ni_4Ti_3 phase occurs during furnace cooling from HIP temperature. A more detailed discussion of this phenomenon can be found elsewhere (Ref 33). Therefore, phase transformation behavior of all NiTi and NiTi-X alloys prepared in this study was investigated after solution treatment at 950 °C for 1 h with subsequent water quenching.

After solution treatment, martensitic phase transformation of powder metallurgical Ni50.8Ti49.2 alloy is characterized by $M_S = -9$ °C, $M_P = -17$ °C, and $M_F = -26$ °C. The transformation back to austenite took place at $A_S = +10$ °C, $A_P = +23$ °C and $A_F = +27$ °C. As expected, single-step phase transformations were found in both cases. The hysteresis between M_P and A_P was 40 °C after solution treatment. According to Frenzel et al.'s study (Ref 5), the phase transformation temperatures are related to a Ni-content in the range of 50.8-50.9 at.% Ni. The trend of slight increase of Ni content compared with NiTi rod used as starting material might be explained by uptake of oxygen and carbon during processing, mainly during gas atomization. This uptake is coupled with the formation of oxygen-containing Ti_2Ni and TiC phases with increasing Ni content of NiTi matrix (Ref 5, 36). A detailed discussion of these phases in the case of powder metallurgical processing can be found elsewhere (Ref 33, 34, 36). Owing to the strong influence of solution treatment on phase transformation temperature and hysteresis found for binary NiTi alloys, solution treatment was also applied for all NiTi-X (X = Nb, Ag, W) samples.

3.3 NiTi-Nb Alloys

Figure 3 shows the microstructure of the NiTi-3Nb alloy. It is supposed that the formation of eutectic melt, which forms at temperatures above 1170 °C (Ref 16, 22), does not take place as HIP cycle was conducted at 1065 °C. Therefore, the main mechanisms of densification were solid-state diffusion in combination with plastic flow. The latter is caused by superposition of pressure during sintering. Energy-dispersive X-ray analysis (EDX) was performed to investigate the composition of the apparent phases marked in Fig. 3 (related EDX spectra not shown here). As expected, the alloy consists of ductile Nb phase, which contains significant amount of Ti (1), an obviously brittle phase with several cracks containing Ti, Ni, Nb, and O (likely $Ti_4(Ni,Nb)_2O_x$), which surrounds the Nb phase as a shell (2) and the NiTi matrix, which contains a significant amount of Nb (3).

The formation of Nb-containing NiTi matrix and Ti-containing Nb phases were also described in the literature for NiTi-Nb alloys made by liquid-phase sintering (Ref 16) and ingot metallurgy (Ref 15). At 900 °C, the Nb-containing NiTi matrix and Ni_2Ti phase are in equilibrium (Ref 16). Depending on the exact alloy composition, different phase compositions like $(Ti,Nb)_4Ni_2O$, $(Ti_3Ni,Nb)_2$ or $(Ni,Nb)_3Ti$ are reported are reported in the literature (Ref 39).

Furthermore, some isolated gray dots are visible in the NiTi matrix, which are supposed to be oxygen-containing Ti_2Ni and TiC phases as well known from binary NiTi alloys. The contents of these oxides and carbides in the NiTi matrix are lower than those expected from the results of chemical analysis (see Table 2). Therefore, it is concluded that most of the oxygen atoms introduced by the Nb phase are still dissolved in this phase or consumed by the formation of the oxide shell surrounding the Nb-phase.

Figure 4 compares the phase transformation behavior of the NiTi-3Nb and NiTi-9Nb alloys with the DSC results of the prealloyed Ni50.8Ti49.2 sample. Here, Fig. 4(a) shows the austenitic phase transformation during heating, and Fig. 4(b) the martensitic phase transformation during cooling. As mentioned, all the samples were solution treated.

Contrary to the results reported in the literature for NiTi-Nb alloys prepared with varying Nb contents by ingot metallurgy [4.5-30 at.% Nb (Ref 13, 15, 40, 41)], powder metallurgical NiTi-3Nb sample showed an increase of transformation temperatures compared to Ni50.8Ti49.2 alloy, which was quite unexpected. After increasing the Nb-content to 9 at.% (NiTi-9Nb), the expected temperature shift to lower values tends to start. Nevertheless, even these temperature values are even higher than the transformation temperatures of the binary NiTi alloy. Unfortunately, weakly pronounced transformation peaks hamper exact characterization of phase transformation behavior. A discussion of temperature hysteresis depending on Nb-content is given later.

This unexpected phase transformation behavior was reproduced with NiTi-3Nb, NiTi-5Nb, NiTi-7Nb and NiTi-9Nb samples, which were produced by warm pressing using same starting powders. Warm pressing is used at our institute for simulating the MIM process if only small powder batches are available (Ref 42). For warm pressing, a binary binder system based on paraffin, and polyethylene (ratio 60:40) was proven for MIM processing of powders with high affinity to oxygen and carbon. Parameters of warm pressing can be found elsewhere (Ref 42). Even in the case of warm-pressed samples,

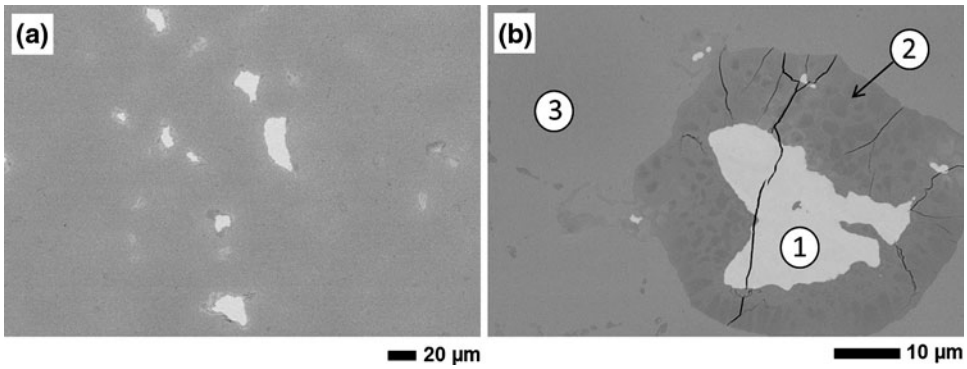

Fig. 3 Microstructure of NiTi-3Nb after HIP processing (1065 °C, 100 MPa, 3 h): (a) Overview, and (b) EDX analysis: Nb phase with Ti in solid solution (1); probably ($Ti_4(Ni,Nb)_2O_x$), formation of cracks indicates the brittle nature (2); and NiTi matrix with Nb in solid solution (3)

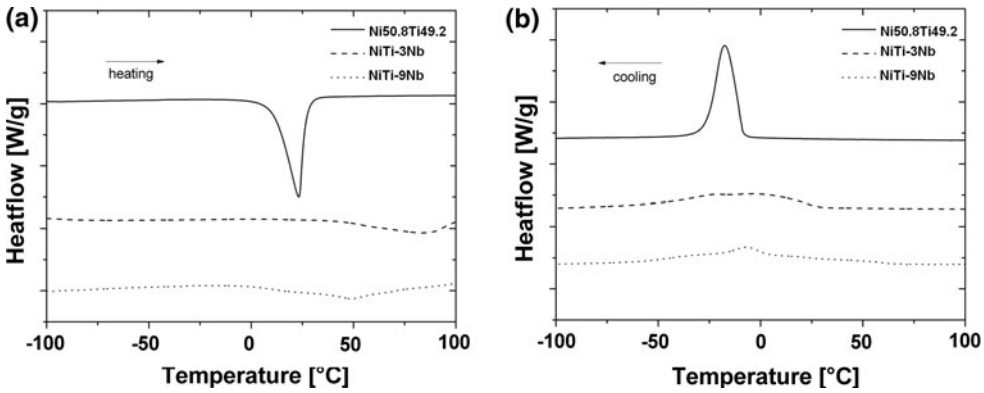

Fig. 4 DSC measurements of NiTi-3Nb and NiTi-9Nb alloys compared with Ni50.8Ti49.2 reference, with all samples being compacted by HIP (1065 °C, 100 MPa, 3 h) with subsequent solution treatment (950 °C, 1 h, quenching in water). (a) Austenitic phase transformation during heating, and (b) martensitic phase transformation during cooling

increase of phase transformation temperatures was found at Nb-content of 3 at.% (measurement results not shown here). The expected shift to lower phase transformation temperatures occurred not until the Nb-content exceeded 5 at.%.

3.4 NiTi-Ag Alloys

Figure 5 shows the microstructure of NiTi-3Ag alloy. As expected from low melting temperature of Ag (961 °C), Ag-particles appear to be completely molten during the HIP cycle, which is indicated by complete filling of all gaps between spherical NiTi particles. Pure Ag-phase (1) surrounded by NiTi matrix (2) was observed in the NiTi-Ag alloy. No indication of interdiffusion was found. In the NiTi matrix, formation of TiC phase visible as black dots (3) and oxygen-containing Ti_2Ni phase visible as light gray phase (4) occurred as already known from binary NiTi (Ref 5, 32-34, 36). Owing to the low oxygen and carbon contents of the Ag powder used as starting material, the oxygen and carbon levels remained almost constant when comparing Ni50.8Ti49.2, NiTi-3Ag, and NiTi-9Ag samples (see Table 2).

If measuring the phase transformation temperatures by DSC, it becomes obvious that the addition of Ag decreases the temperatures for martensitic as well as austenitic phase transformation (Fig. 6). The temperature shift becomes enlarged with increasing Ag-content.

3.5 NiTi-W Alloys

Contrary to NiTi-Nb and NiTi-Ag alloys, W powder particles remained almost unchanged after HIP of NiTi-3W and NiTi-9W (Fig. 7). This behavior was not unexpected considering the high melting point (T_m = 3422 °C) and brittleness of W particles. Nevertheless, all W particles were completely embedded in the NiTi matrix demonstrating the occurrence of plastic flow during HIP. Analyzing phase composition by EDX hints on a slight tendency of Ni diffusion into the W particles (1), but this result might be influenced by presence of NiTi in the gaps of agglomerated W particle clusters. In the NiTi matrix (2), there was no indication of W diffusion into NiTi. Again, oxygen and carbon contamination of the NiTi matrix led to formation of oxygen-containing Ti_2Ni (light gray dots) and TiC (black dots) phases as marked by arrows (3). The oxygen and carbon contents of the NiTi-3W and NiTi-9W alloys were increased significantly, which was expected from impurity contents of the W powder. As there is almost no solubility of oxygen in W (Ref 43), it is supposed that the increased oxygen content might cause an increased content of oxygen-containing Ti_2Ni phase in the NiTi matrix. If this effect would happen, the formation of this phase should preferentially occur in vicinity of the W clusters. Up to now, this assumption could not be confirmed by metallography. Contrary to the negligible solubility of oxygen, W exhibits

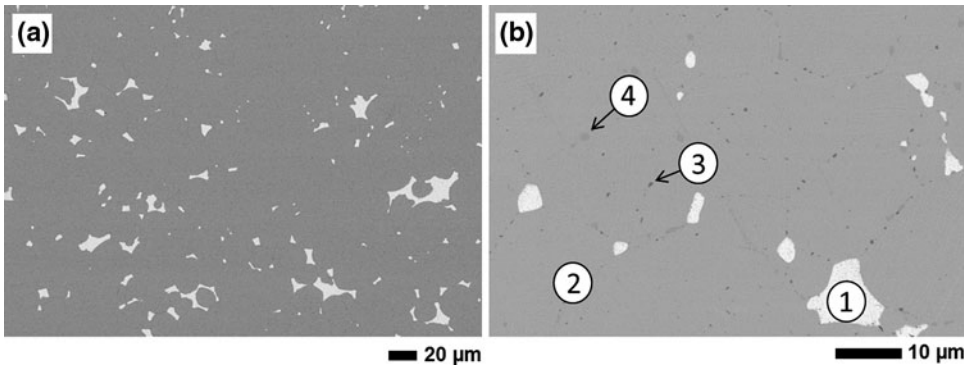

Fig. 5 Microstructure of NiTi-3Ag after HIP processing (1065 °C, 100 MPa, 3 h): (a) Overview, and (b) EDX analysis: pure Ag phase (1), NiTi matrix (2), TiC visible as small black dots (3), oxygen-containing Ti2Ni phase being visible also as small light gray dots (4)

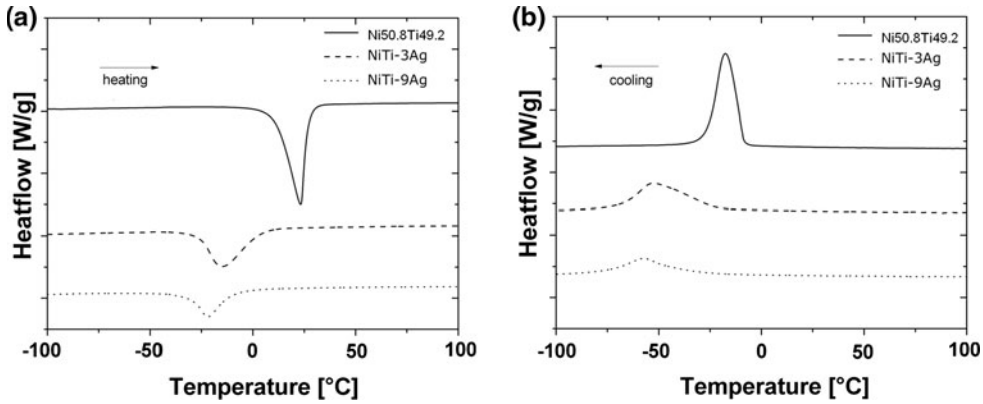

Fig. 6 DSC measurements of NiTi-3Ag and NiTi-9Ag alloys compared with Ni50.8Ti49.2 reference, with all the samples being compacted by HIP (1065 °C, 100 MPa, 3 h) with subsequent solution treatment (950 °C, 1 h, quenching in water): (a) Austenitic phase transformation during heating, and (b) martensitic phase transformation during cooling

significant solubility of carbon of up to 1 at.% (Ref 44). Even if solution of such amounts requires temperatures higher than 1000 °C, it can be assumed that the low C content detected in the W powder (<0.001 at.%) stays in solid solution even after HIP processing. Therefore, the increase of TiC phase content due to adding elemental W powder could be neglected in the present study.

The phase transformation behavior of NiTi-3W and NiTi-9W compared with Ni50.8Ti49.2 reference is shown in Fig. 8. Again, the addition of W is coupled with a shift of transformation temperatures to lower values. Phase transformation temperatures follow the same trend as already found in the case of adding elemental Ag powders, even if these elements should act quite different considering their large differences in strength and ductility. A more detailed discussion of this result is given in the next section.

4. Discussion of Influence of Nb, Ag, and W Additions on Phase Transformation

Table 4 summarizes phase transformation temperatures of all alloys investigated in this study. For excluding the influence of Ni_4Ti_3 precipitations on phase transformation behavior, all the samples were solution annealed (950 °C, 1 h, water quenching) before DSC measurement. In the case of Ni50.8Ti49.2 reference, the temperature hysteresis between A_P and M_P is in the same range as expected from the literature. Based on the results published by Frenzel et al. (Ref 5), a temperature hysteresis of 38 °C was expected for the given alloy composition.

4.1 NiTi-Nb

Based on several studies done on NiTi-Nb alloys made by ingot metallurgy (Ref 13, 15, 40), continuous decrease of phase transformation temperatures with increasing Nb content is expected. In the present study, an unexpected shift of phase transformation temperatures in opposite direction to higher values was observed, especially at low Nb contents. Broadening of temperature hysteresis tends to occur for both alloy compositions (NiTi-3Nb, NiTi-9Nb), but exact determination of this effect was hampered by weakly pronounced transformation peaks (Fig. 4). Nevertheless, the observed transformation behavior suggests the occurrence of multistep phase transformations. The shift to higher temperatures could be reproduced if the same alloy compositions were prepared by warm pressing as already mentioned in "NiTi-Nb Alloys" section.

The unexpected increase of phase transformation temperatures especially at low Nb contents might be explained by the occurrence of solid-state diffusion processes of Nb into NiTi

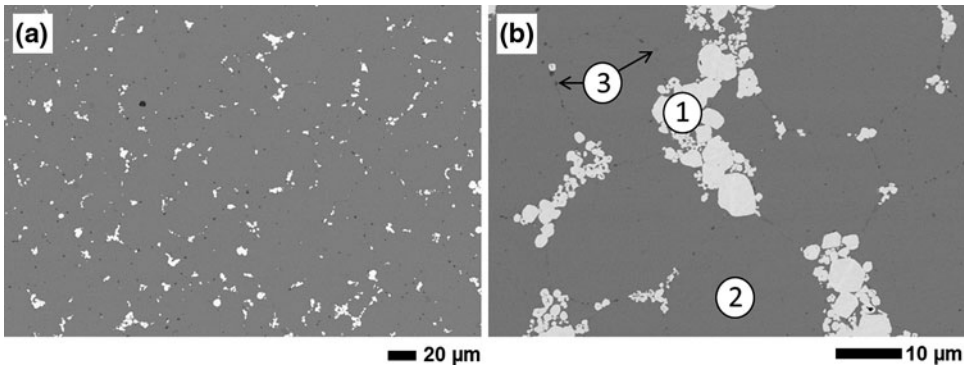

Fig. 7 Microstructure of NiTi-3W after HIP processing (1065 °C, 100 MPa, 3 h). (a) Overview and (b) EDX analysis: W phase with indication of rather small Ni content in solid solution (1), NiTi matrix without W (2), oxygen-containing Ti2Ni and TiC as light gray and black dots (3)

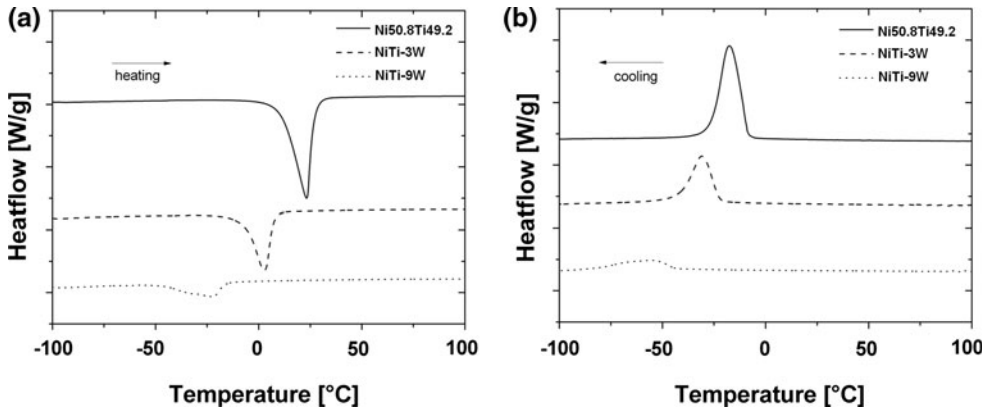

Fig. 8 DSC measurements of NiTi-3W and NiTi-9W alloys compared with Ni50.8Ti49.2 reference, showing all samples compacted by HIP (1065 °C, 100 MPa, 3 h) with subsequent solution treatment (950 °C, 1 h, quenching in water). (a) Austenitic phase transformation during heating, and (b) martensitic phase transformation during cooling

Table 4 Summary of phase transformation temperatures and hysteresis between martensitic and austenitic phase transformations for ternary NiTi-X (X = Nb, Ag, and W) alloys compared with binary Ni50.8Ti49.2 alloy

Alloy	M_S	M_P	M_F	A_S	A_P	A_F	Hysteresis $A_P - M_P$, °C
Ni50.8Ti49.2	−8	−17	−26	+11	+23	+28	40
NiTi-3Nb	+30*	−3*	−51*	+34*	+84*	+105*	87*
NiTi-9Nb	+16*	−7*	−30*	+9*	+49*	+82*	56*
NiTi-3Ag	−19	−53	−70	−27	−14	+6	39
NiTi-9Ag	−34	−57	−75	−32	−22	−8	35
NiTi-3W	−22	−31	−42	−7	+2	+7	33
NiTi-9W	−44	−56	−85	−48	−22	−16	34

All alloys were prepared by HIP (1065 °C, 100 MPa, 3 h) with subsequent solution treatment (950 °C, 1 h, water quenching)
* Exact determination of these values influenced by weakly pronounced peaks

matrix and Ti into Nb particles which led to concentration profiles that differ significantly from NiTi-Nb alloys prepared by ingot metallurgy. Furthermore, the formation of $(Ni,Nb)_3Ti$ phase, which is thermodynamically stable for the given composition as reported in the literature (Ref 46), might cause the shift of transformation temperatures to higher values by changing the Ni:Ti ratio to lower Ni-concentration in the matrix. For further clarification, quantitative EDX and XRD analyses are in progress. In the study of Bansiddhi et al. (Ref 16), NiTi-3Nb alloy was prepared by powder metallurgical means using liquid-phase sintering. In this study, the expected shift of phase transformation temperatures to lower values and the increase of hysteresis from 42 °C (binary NiTi) to 55 °C (NiTi-3Nb) were found. Here, substoichiometric Ni amounts of prealloyed NiTi starting powder (48.6 at.% Ni) excludes formation of (Ni,Nb)3Ti phase (Ref 16).

In the present study, the introduction of high oxygen contents by the Nb phase (Table 2) and formation of core-shell

structure seems to be of less importance, as we found a comparable shift to higher temperatures in NiTi-9Nb alloy, which was recently produced on purpose with same HIP parameter set but starting from significantly less contaminated Nb powder [Nb powder: 0.1760 wt. % O, <0.002 wt. % C; Ni50.6Ti49.4-powder: 0.04 wt. % O, 0.02 wt. % C; NiTi-9Nb alloy (HIP): 0.0684 wt. % O, 0.0248 wt. % C].

4.2 NiTi-Ag and NiTi-W

In the case of adding elemental Ag and W, significant temperature shifts to lower values were observed, which increased with increasing contents of these elements. For comparison, a shift to lower temperatures was also reported in the literature for NiTi-1W and NiTi-2W alloys, which were produced by arc melting (Ref 23). Here, hardening of NiTi matrix due to the W particles, impeding the transformation shear, is discussed as a possible reason. A similar result was reported for NiTi-W coatings prepared by DC sputtering (Ref 25). Here, W particles are discussed to pin grain boundaries. In consequence, reduction of grain size is coupled with reduction of phase transformation temperatures. Contrary to NiTi-W coatings, transformation temperatures of NiTi-Ag coatings produced by DC magnetron sputtering differed not significantly from those of binary NiTi (Ref 24).

The results of our study indicate that martensitic phase transformation is obviously hampered both in NiTi-Ag and NiTi-W alloys probably because of pinning of the transformation front. From thermodynamic point of view, higher degrees of undercooling are required for proceeding of martensitic phase transformation resulting in lowered phase transformation temperatures. On the other hand, during subsequent heating stabilization of martensite by these phases seems to be unlikely as there was obviously no broadening of temperature hysteresis as described in the literature for NiTi-Nb alloys even for undeformed alloys (Ref 13). Such broadening could be expected at least in the case of adding elemental Ag, as high ductility of this alloying element should allow plastic deformation of Ag at the NiTi-Ag interface facilitating accommodation of surrounding martensite. Our results do not indicate such effect.

In addition to the pinning effect described above, it may be assumed that also stresses around the insoluble alloying phases could influence shift of phase transformation temperatures. For example, in the case of formation of metastable Ni_4Ti_3 precipitations in Ni-rich NiTi alloys, it is well known that stresses around precipitations promote the formation specific orientations of martensite as well as occurrence of double- or multistage phase transformation including the trigonal R-phase (Ref 37, 45). In previous study, even powder metallurgical Ni50.8Ti49.2 showed this strong dependency of R-phase as well as austenite-martensite phase transformation temperatures on the annealing temperature (investigated temperature range 430-630 °C, 1 h) and therefore on size of Ni_4Ti_3 precipitations (Ref 33). In the present study, this effect was excluded reliably, as all the samples were solution treated (950 °C, 1 h, water quenching). Nevertheless, significant deviations of TEC between NiTi matrix and elemental Ag as well as W phase might induce stresses at the NiTi-Ag or NiTi-W interface, which could promote formation of preferred orientations of martensite similar to the effect introduced by Ni_4Ti_3 precipitates. If this assumption would be correct, then higher TEC of Ag compared with NiTi should lead to tensile stresses in the surrounding NiTi matrix, while W additions should promote compression stresses because of lower TEC compared to NiTi. Therefore, different trends of temperature shift are expected in NiTi-Ag and NiTi-W alloys if considering the influence of TEC mismatch. For clarification, TEM investigations at the interface NiTi-Ag and NiTi-W would be of high interest to see if increased dislocation densities might appear in Ag, W or NiTi for stress release.

When comparing NiTi-Ag and NiTi-W, the more pronounced temperature shift in the case of W additions might be further explained by the higher oxygen contents introduced by the W phase. As there is almost no solubility of oxygen in elemental W, an increase of oxygen-containing Ti_2Ni phase in NiTi matrix should arise with increasing W content, which enlarges the temperature shift because of increasing Ni-content of NiTi matrix. On the other hand, microstructural investigation

Table 5 Widening of coupling rings made of Ni50.8Ti49.2 and NiTi-X (X = Nb, Ag, W) alloys in liquid nitrogen

Alloy	6% expansion	12% expansion
Ni50.8Ti49.2	✓	Failed
NiTi-3Nb	✓	✓
NiTi-9Nb	✓	Failed
NiTi-3Ag	✓	Failed
NiTi-9Ag	✓	Failed
NiTi-3W	✓	Failed
NiTi-9W	Failed	Failed

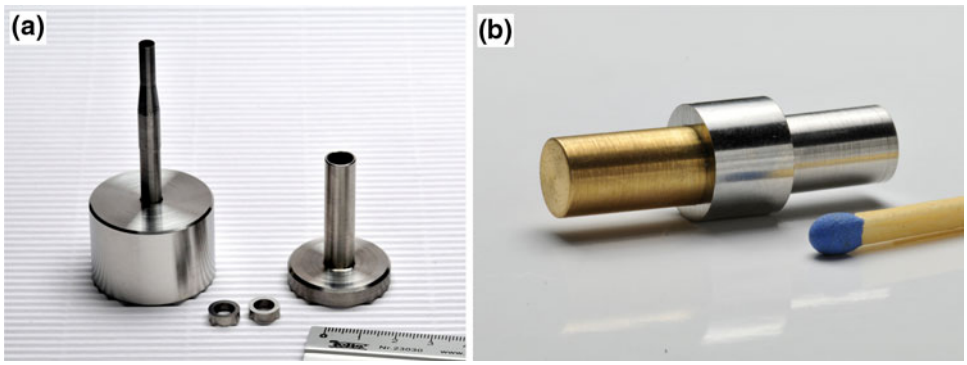

Fig. 9 (a) Device for widening NiTi-X rings produced by HIP and wire cut EDM and (b) proof of function

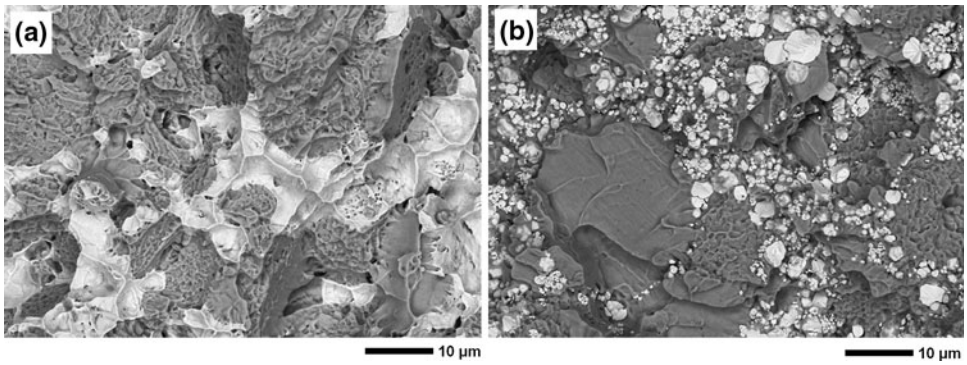

Fig. 10 Fractured surface of couplings rings made of NiTi-9Ag (a) and NiTi-9W (b), which failed after expansion to 12%. Dark phase: NiTi matrix; bright phase: Ag (a) and W (b)

(see Fig. 7) did not prove this assumption as no increase of Ti_2Ni phase was found in the vicinity of W phase.

5. Manufacturing of Coupling Rings for Prove of Function

For demonstration of manufacturing net-shaped parts from these alloys and the proof of their function, prototypes of coupling rings were produced by wire cut EDM from HIP samples. Afterward, they were expanded up to 6 and 12% in liquid nitrogen, using the device shown in Fig. 9(a). With the exception of the NiTi-9W alloy, all samples showed sufficient ductility to expand them up to 6% (Table 5). Furthermore, complete shape recovery due to the one way shape memory effect was observed in all cases, when the samples were heated above the austenite finish temperature. When increasing the expansion to 12%, all samples failed by fracture with exception of NiTi-3Nb sample, but even for this sample, incomplete shape recovery of only 50% was observed indicating the need for further improvement of processing technology and subsequent thermal treatments to become competitive to coupling rings produced by ingot metallurgy.

Fractured surface of couplings rings made of NiTi-9Ag and NiTi-9W, which failed after expansion to 12%, was investigated by SEM to estimate the adherence of the Ag and W phases to the NiTi matrix (Fig. 10). In the case of Ag addition, ductile fracture of Ag particles suggests good interfacial bonding of this phase to the NiTi matrix. Vice versa, W particles tend to be weakly bonded to the NiTi matrix, which is not unexpected considering the lack of interdiffusion process during HIP.

6. Summary and Outlook

Ternary NiTi-X (X = Nb, Ag, and W) alloys were produced from prealloyed Ni50.8Ti49.2 powders with addition of elemental Nb, Ag, and W powders by HIP (1065 °C, 100 MPa, 3 h) with subsequent solution treatment (950 °C, 1 h). For reference, samples from binary Ni50.8Ti49.2 were prepared using the same parameter set, which showed phase transformation behavior as expected from a previous study. When adding elemental Nb, shift of phase transformation behavior to higher values was observed. This result is contrary to results in the literature achieved on NiTi-Nb alloys, which were prepared by ingot metallurgy or by sintering with transient liquid phase. It is proposed that the differences in phase composition due to solid-state sintering (e.g., deviation of Nb content in the NiTi matrix) are responsible for this result. In the case of addition of elemental Ag or W, shift of phase transformation temperatures to lower values was observed in both cases, which increased with amount of ternary alloying element. Here, it was thought that the proceeding of martensite transformation was hindered by Ag or W inclusions in the NiTi matrix requiring increased undercooling to achieve fully pronounced martensitic phase transformation. In our investigation there was no clear indication of broadening the hysteresis of austenite-martensite phase transformation temperatures due to the addition of these low soluble oder almost insoluble alloying phases. First, attempts were conducted to demonstrate the functionality of these alloys on coupling rings, which were expanded to 6 and 12%.

As the shift of phase transformation temperatures, as well as failure of rings at 12% expansion (exception NiTi-3Nb), is not fully understood yet, the following investigations are in progress:

- Microhardness measurement of all phases
- For NiTi-Nb alloys: Quantitative analysis of Nb content in NiTi as well as Ti content in Nb phase
- Investigation of mechanical properties under tensile load
- DSC measurement of rings after deformation to see the influence of plastic deformation of alloying phase on temperature hysteresis
- TEM investigation of NiTi-Ag and NiTi-W interface
- Metal injection moulding MIM of NiTi-Nb and NiTi-Ag alloys combined with sintering with transient liquid phase

Acknowledgments

This study was financially supported by the Deutsche Forschungsgemeinschaft (DFG) within the research centre SFB 495 (shape memory technology) of Ruhr-Universität Bochum. Financial supports as well as contributions of Dr. D. Sebold (SEM images) and Mr. D. Rose (DSC-measurements) are gratefully acknowledged.

References

1. S. Saito, T. Wachi, and S. Hanada, A Study on the Machinability of a Ti Ni Shape Memory Alloy, *Mater. Sci. Eng.*, 1992, **161**, p 91–96
2. Y. Furuya, A. Sasaki, and M. Taya, Enhanced Mechanical Properties of TiNi Shape Memory Fiber/Al Matrix Composite, *Mater. Trans. JIM*, 1993, **34**, p 224–227
3. M. Taya, Y. Yamamda, R. Watanabe, S. Shibata, and T. Mori, Strengthening Mechanism of TiNi Shape Memory Fiber/Al Matrix Composite, *SPIE*, 1992, **1916**, p 373–383
4. S. Miyazaki, K. Otsuka, and Y. Suzuki, Transformation Pseudoelasticity and Deformation Behavior in a Ti-506 at% Ni Alloy, *Scr. Metall. Mater.*, 1981, **15**, p 287–292
5. J. Frenzel, E.P. George, A. Dlouhy, C. Somsen, M.X.F. Wagner, and G. Eggeler, Influence of Ni on Martensitic Transformations in NiTi Shape Memory Alloys, *Acta Mater.*, 2010, **58**, p 3444–3458
6. T.H. Nam, D.W. Chung, J.P. Noh, and H.W. Lee, Phase Transformation Behavior and Wire Drawing Properties of Ti-Ni-Mo Shape Memory Alloys, *J. Mater. Sci.*, 2001, **36**, p 4181–4188
7. T. Kurita, H. Matsumoto, K. Sakamoto, K. Tanji, and H. Abe, Effect of Aluminium on the Transformation of NiTi Alloy, *J. Alloys Comp.*, 2005, **396**, p 193–196
8. S. Besseghini, E. Villa, and A. Tuissi, NiTiHf Shape Memory Alloy: Effect of Aging and Thermal Cycling, *Mater. Sci. Eng.*, 1999, **A273–275**, p 390–394
9. H. Hosoda et al., Martensite Transformation Temperatures and Mechanical Properties of Ternary NiTi Alloy with Offstoichiometric Compositions, *Intermetallics*, 1998, **6**, p 291–301
10. F.J. Gil and J.A. Planell, Thermal Efficiencies of NiTiCu Shape Memory Alloys, *Thermochim. Acta*, 1999, **327**, p 151–154
11. W. Siegert et al., Influence of Nb Content and Processing Conditions on Microstructure and Functional Properties of NiTiNb Shape-Memory Alloys, *Mater. Sci. Forum*, 2002, **394–395**, p 361–364
12. V. Petzoldt, Formgedächtnistechnik Tiefbohren und Mikrofräsen von NiTi: Schriftenreihe ISF 2006
13. T.W. Duerig and K.N. Melton, Wide Hysteresis NiTiNb Alloys, *The Martensitic Transformation in Science and Technology*, E. Hornbogen and N. Jost, Ed., DGM Informationsgesellschaft mbH, Oberursel, 1989, p 191–198
14. C.S. Zhang et al., Effects of Deformation on the Transformation Hysteresis and Shape Memory Effect in a $Ni_{47}Ti_{44}Nb_9$ Alloy, *Scr. Metall. Mater.*, 1990, **24**, p 1807–1812
15. L.C. Zhao, T.W. Duerig, S. Justi, K.N. Melton, J.L. Proft, W. Yu, and C.M. Wayman, The Study of Niobium-Rich Precipitates in a NiTiNb Shape Memory Alloy, *Scr. Metall.*, 1990, **24**, p 221–225
16. A. Bansiddhi and D.C. Dunand, Shape-Memory NiTi-Nb Foams, *J. Mater. Res.*, 2009, **24**, p 2107–2117
17. T. Wu and M.H. Wu, NiTiNb Plugs for Sealing High Pressure Fuel Passages in Fuel Injector Applications, in *Proceedings of International Conference on Shape Memory and Superelastic Technologies (SMST 2000)*, Pacific Grove, CA, USA, 2000, p 235–240
18. X. Zhao, X. Yan, Y. Yang, and H. Xu, Wide Hysteresis NiTi(Nb) Shape Memory Alloys with Low Nb Content (4.5 at.%), *Mater. Sci. Eng. A*, 2006, **438–440**, p 575–578
19. K.T. Oh, U.K. Joo, G.H. Park, C.J. Hwang, and K.N. Kim, Effect of Silver Addition on the Properties of Nickel-Titanium Alloys for Dental Application, *J. Biomed. Mater. Res. B*, 2006, **76**, p 306–314
20. H. Enami, M. Hara, and H. Maeda, Effect of W Addition on the Martensitic Transformation and Shape Memory Behavior of the TiNi-Base Alloy, *J. Phys. IV Fr.*, 1995, **5**(C8), p 629–633
21. X.J. Yan, H. Gugel, S. Huth, and W. Theisen, Microstructures and Properties of Laser Cladding NiTi Alloy with W for Biomedical Applications, *Mater. Lett.*, 2011, **65**, p 2934–2936
22. D.S. Grummon, J.A. Shaw, and J. Foltz, Fabrication of Cellular Shape Memory Alloy Materials by Reactive Eutectic Brazing Using Niobium, *Mater. Sci. Eng. A*, 2006, **438**, p 1113–1118
23. S.F. Hsieh, S.K. Wu, H.C. Lin, and C.H. Yang, Transformation Sequence and Second Phases in Ternary Ti-Ni-W Shape Memory Alloys with Less Than 2 at% W, *J. Alloys Comp.*, 2005, **387**, p 121–127
24. C. Zamponi, M. Wuttig, and E. Quandt, Ni-Ti-Ag Shape Memory Thin Films, *Scr. Mater.*, 2007, **56**, p 1075–1077
25. P.J.S. Buenconsejo, R. Zarnetta, and A. Ludwig, The Effects of Grain Size on the Phase Transformation Properties of Annealed (Ti/Ni/W) Shape Memory Alloy Multilayers, *Scr. Mater.*, 2011, **64**, p 1047–1050
26. P.J.S. Buenconsejo, A. Siegel, A. Savan, S. Thienhaus, and A. Ludwig, Preparation of 24 Ternary Thin Film Materials Libraries on a Single Substrate on One Experiment for Irreversible High-Throughput Studies, *ACS Combin. Sci.*, 2012, **14**, p 25–30
27. http://jmmedical.com/resources/221/Nitinol-Technical-Properties.html. Accessed 15 April 2012
28. http://www.goodfellow.com/E/Niobium.html. Accessed 15 April 2012
29. http://www.goodfellow.com/E/Silver.html. Accessed 15 April 2012
30. http://www.goodfellow.com/G/wolfram.html. Accessed 15 April 2012
31. L. Krone, J. Mentz, M. Bram, H.P. Buchkremer, D. Stöver, M. Wagner, G. Eggeler, D. Christ, S. Reese, D. Bogdanski, M. Köller, S.A. Esenwein, G. Muhr, O. Prymak, and M. Epple, The Potential of Powder Metallurgy for the Fabrication of Biomaterials on the Basis of Nickel-Titanium: A Case Study with a Staple Showing Shape Memory Behaviour, *Adv. Eng. Mater.*, 2005, **7**, p 613–619
32. J. Mentz, J. Frenzel, M.F.X. Wagner, K. Neuking, G. Eggeler, H.P. Buchkremer, and D. Stöver, Powder Metallurgical Processing of NiTi Shape Memory Alloys with Elevated Transformation Temperatures, *Mater. Sci. Eng. A*, 2008, **491**, p 270–278
33. M. Bram, M. Bitzer, H.P. Buchkremer, and D. Stöver, Reproducibility Study of NiTi Parts Made by Metal Injection Moulding, *J. Mater. Eng. Perf.*, 2012. doi:10.1007/s11665-012-0264-6
34. J. Mentz, M. Bram, H.P. Buchkremer, and D. Stöver, Improvement of Mechanical Properties of Powder Metallurgical NiTi Shape Memory Alloys, *Adv. Eng. Mater.*, 2006, **8**, p 247–252
35. J. Mentz, L. Krone, M. Bram, H.P. Buchkremer, and D. Stöver, Influence of Heat Treatment on Properties of Hot Isostatic Pressed (HIP) NiTi, *Int. Conference on Shape Memory and Superelastic Technologies, SMST*, 3-7 October 2004, Baden–Baden, Germany, 2006, p 489–494
36. J. Mentz, M. Bram, H.P. Buchkremer, D. Stöver, Improvement of Mechanical Properties of Powder Metallurgical NiTi by Reduction of Impurity Phases, *International Conference on Shape Memory and Superelastic Technologies SMST*, 7-11 May 2006, B. Berg, M.R. Mitchell, J. Proft, Eds., Pacific Grove, CA, USA, 2008, p 399–408
37. J. Khalil-Allafi, A. Dlouhy, and G. Eggeler, Ni_4Ti_3-Precipitation During Aging of NiTi Shape Memory Alloys and Its Influence on Martensitic Phase Transformations, *Acta Mater.*, 2002, **50**, p 4255–4274
38. W. Tang, B. Sundmann, R. Sandström, and C. Quiu, New Modelling of the B2 Phase and its Associated Martensitic Transformation in the Ti-Ni System, *Acta Mater.*, 1999, **47**, p 3457–3468
39. J. Di, L. Wen-xi, D. Zhr-zhong, H. Ming, and W. De-fa, Influence on Phase Composite and Mechanical Properties of $Ni_{47}Ti_{44}Nb_9$ Alloy, *Trans. Nonferrous Met. Soc. China*, 2003, **13**, p 917–921
40. W. Siegert, K. Neuking, M. Mertmann, and G. Eggeler, First Cycle Shape Memory Effect in the Ternary NiTiNb System, *J. Phys. IV Fr.*, 2003, **112**, p 739–742
41. M. Piao, K. Otsuka, S. Miyazaki, and H. Horikawa, Mechanism of the As Temperature Increase by Pre-deformation in Thermoelastic Alloys, *Mater. Trans. JIM*, 1993, **10**, p 919–929
42. A.P. Cysne Barbosa, M. Bram, H.P. Buchkremer, and D. Stöver, Fabrication of Titanium Implants with a Gradient in Porosity by 2-Component MIM, *Powder Inject. Mould. Int. PIM*, 2012, **6**, p 69–73
43. H.A. Wriedt, The O-W (Oxygen-Tungsten) System, *Bull. Alloy Phase Diagr.*, 1989, **10**, p 368–384
44. H. Okamoto, C-W (Carbon-Tungsten), *J. Phase Equilib. Diffus.*, 2008, **29**, p 543–544
45. K. Otsuka and X. Ren, Physical Metallurgy of Ti-Ni-Based Shape Memory Alloys, *Prog. Mater. Sci.*, 2005, **50**, p 511–678